Semnan University

Journal of Modeling & Simulation in Electrical & Electronics Engineering (MSEEE)
Journal homepage: **https://mseee.semnan.ac.ir/**

ISSN: 2821-0786

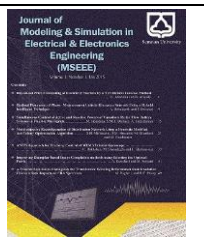

Design, Simulation and Fabrication of MIMO Antenna with Multi-Frequency Coverage a Lot of Different Types of Wireless Communication Systems

Mohamad Hossein Montazerifar [1], Jasem Jamali*[2], Zahra Adelpour[3]

***Abstract*-- This paper presents the design, simulation, fabrication, and testing of a MIMO antenna optimized for wideband applications, with specific suitability for standards such as Bluetooth, Wi-Fi, LTE, and IEEE 802.11 a/b/g/n. The antenna exhibits strong impedance matching over four operating bands: 2.17–2.62 GHz, 3.6–3.8 GHz, 6.68–8.42 GHz, and 8.85–24.85 GHz. The design incorporates a parasitic element to enhance isolation and reduce mutual coupling between 1×2 antenna elements, achieving an isolation level exceeding 21 dB across the operating bands. Simulated and measured results are in close agreement, with minor deviations attributed to fabrication tolerances and connector losses. The antenna maintains a stable gain between 3.9 dB and 6.9 dB, demonstrating excellent omnidirectional and bidirectional radiation patterns in the E-plane and H-plane, respectively. These results confirm the antenna's potential for use in modern wireless communication systems requiring compact designs, high isolation, and wideband performance.**

Keywords: MIMO Antenna, Wideband, Parasitic Element, Mutual Coupling, Isolation.

I. INTRODUCTION

In recent years, the rapid growth in the demand for high-speed data transmission and efficient communication systems has spurred the development of various technologies aimed at increasing the data rate and the volume of transmitted information. As communication networks expand to accommodate a growing number of devices and the increasing data demands, the need for efficient and reliable systems has never been more crucial. In particular, the demand for high-capacity systems that can deliver faster data rates while maintaining energy efficiency and minimizing power consumption has led to a growing interest in MIMO (Multiple-Input, Multiple-Output) systems[1]. MIMO systems leverage spatial diversity to increase the overall capacity of a wireless communication system, allowing for the simultaneous transmission of multiple data streams over the same frequency band. This technique enables the transmission of large volumes of data without the need for additional bandwidth or increased power, making it a highly effective solution for meeting the growing demand for high-speed data transmission. As a result, MIMO systems have become a key technology in various modern wireless communication standards, including 4G and 5G networks, WiFi, Bluetooth, and more[2].

Designing MIMO antennas involves two primary challenges: minimizing antenna size and ensuring sufficient isolation between ports. To address these challenges, various methods have been explored in the literature. These include optimizing antenna geometries [3,4], employing metamaterial structures [5-7], incorporating decoupling networks [8,9], the neutralization line [10], the defected ground structure (DGS) [11,12], and the dual-polarized antenna [13,14].

In recent years, significant research has been conducted to design MIMO antennas with wide impedance bandwidth, improved isolation, and compact size for various applications. For instance, a MIMO antenna with four elements was proposed for UWB systems, incorporating a U-shaped slot on the radiating patch to achieve a band-notch characteristic at 5.5 GHz for WLAN. The antenna elements

Received; 2025-07-28 Revised; 2025-10-12 Accepted; 2025-10-28

[1] Department of Electrical Engineering, Ma.c, Islamic Azad University, Mashhad, Iran.
[2] Department of Electrical Engineering, Islamic Azad University, Kazerun, Iran.
[3] Department of Electrical Engineering, Islamic Azad University, Shiraz, Iran.
* Corresponding author Email: jasem.jamali@iau.ac.ir

Cite this article as:
Montazerifar, M,H., Jamali, J.,& Adelpour, Z. (2025). Design, Simulation and Fabrication of MIMO Antenna with Multi-Frequency Coverage a Lot of Different Types of Wireless Communication Systems. *Journal of Modeling & Simulation in Electrical & Electronics Engineering (MSEEE).* Semnan University Press . *5 (3),* 29-36.
DOI: https://doi.org/10.22075/mseee.2025.38483.1223

© 2025 The Author(s). Journal of Modeling & Simulation in Electrical & Electronics Engineering (MSEEE) is published by Semnan University Press. This is an open-access article under the CC-BY 4.0 license. (https://creativecommons.org/licenses/by/4.0/)

were orthogonally arranged, and a parasitic fan-shaped structure was utilized to enhance isolation and antenna gain, achieving gains of up to 7.6 dBi and an ECC below 0.01 across the operating band [15]. Another study utilized Minkowski fractal structures in a MIMO antenna with orthogonal element placement. This design demonstrated excellent isolation through additional strip structures, covering applications such as WiMAX, WLAN, and X-band frequencies with an ECC below 0.005 [16]. Similarly, a CPW-fed four-element MIMO antenna introduced a parasitic structure with a square shape and circular and semicircular slots, leading to enhanced gain and isolation over a broad bandwidth of 3–12.8 GHz [17]. Compact designs have also been explored, such as a two-element monopole-based MIMO antenna with T-shaped structures on the ground plane, achieving a wide bandwidth starting from 3.1 GHz and isolation levels exceeding 15 dB [18,19].

Further advancements in MIMO antenna design approaches to the challenges of multi-band operation. A MIMO antenna with circular patches, wide impedance bandwidth (3–4.5 GHz), with a compact size suitable for portable devices, achieving an ECC of 0.02 [20]. Other researchers proposed a semi-circular patch design fed by stepped microstrip lines, achieving isolation above 20 dB and effective suppression of WLAN bands using complementary slot structures [21]. A distinct elliptical loop design for 5G communications at 60 GHz featured orthogonal arrangement and parasitic structures to enhance isolation, yielding gains around 10 dBi with satisfactory ECC and DG values [22]. Lastly, a multi-element MIMO antenna employed different radiating elements with dual polarization, including a T-shaped patch and a square patch, enabling low ECC (<0.1) and high diversity gain (>9.9 dB) across UWB and low-band 5G frequencies, demonstrating the potential for diverse applications in modern wireless systems [23].

In this paper, we propose a novel design for a MIMO antenna system that addresses the challenges of mutual coupling and isolation between antenna elements, which are critical for optimizing system performance. The design incorporates advanced techniques, including the use of parasitic elements and decoupling structures, to improve isolation and enhance the overall efficiency of the antenna array. We also present detailed simulations and measurements of the antenna's performance across various frequency bands, demonstrating its suitability for high-speed communication systems. The results show that the proposed design meets the stringent requirements of modern wireless standards, providing high isolation, compact size, and efficient performance. This work contributes to the ongoing development of MIMO antenna systems, offering valuable insights for next-generation communication technologies.

II. SINGLE-ELEMENT ANTENNA DESIGN

Printed monopole and planar antennas are among the most effective designs for wide and ultra-wideband applications, due to their omnidirectional radiation pattern supporting optimal performance in both transmitting and receiving modes. The general structure of the proposed printed microstrip antenna is shown in Fig. 1. This design is implemented on an FR-4 substrate with a dielectric constant of 4.4, a loss tangent of 0.02, and a thickness of 1.6 mm. The antenna features a circular patch with a diameter of 3 mm and a 50Ω coplanar waveguide (CPW) feed line with dimensions of 1.6 × 42 × 42 mm.

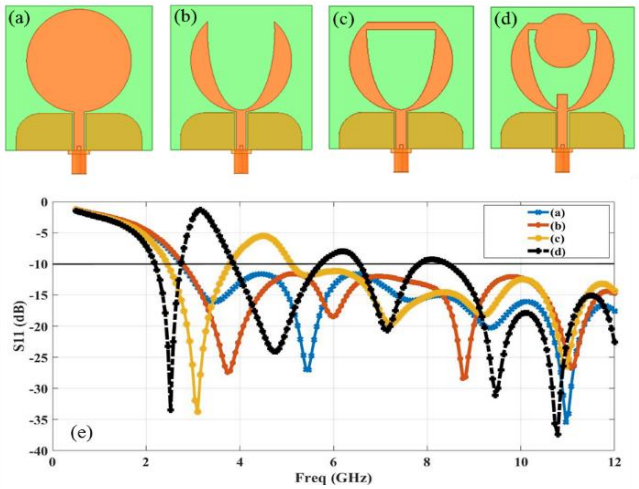

Fig.1.Single-element antenna design ; (a) circular-shaped microstrip patch antenna, (b) elliptical slot, (c) rectangular strip at the top, (d) rectangular strip at the feed position and circular patch at the top, and (e) return loss at each step of antenna design

The proposed antenna's feed line is a 50-ohm CPW type. To achieve a 50Ω input impedance at the antenna's input port, the feed line's length and width were calculated using APPCAD software. The antenna design was initially developed using HFSS software and validated with CST software. Through parameter optimization, optimal values and the final structure of the design were achieved.

The single-element antenna design, as shown in Fig. 1, includes four steps to enable compatibility with multiple frequency bands. The design begins with a circular-shaped microstrip patch antenna, followed by an elliptical slot. Next, a rectangular strip is added to the upper part of the patch, a second rectangular strip is also placed in the feed section, and a circular patch is positioned at the center of the upper strip to support multiple frequency bands. In Fig. 1 (e), the return loss of the single-element antenna is simulated corresponding to each step from (a) to (d). Obviously, each step is associated with better multiband performance. The antenna operates across multiple frequency bands with |S11| < -10 dB, covering ranges of 2.18 – 2.74 GHz, 3.68 – 3.86 GHz, 5.72 – 7.82 GHz, and 8.42 – 24.52 GHz. These frequency ranges allow the antenna to operate in communication standards bands, including Wi-Fi, IEEE 802.11 a/b/g/n, WLAN, Bluetooth, and LTE. The final configuration of the single-element antenna, along with its parameter values, is depicted in Fig. 2 and Table I.

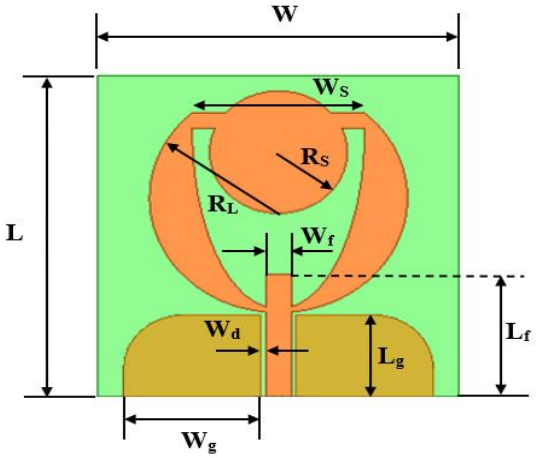

Fig. 2. Configuration of single-element Antenna

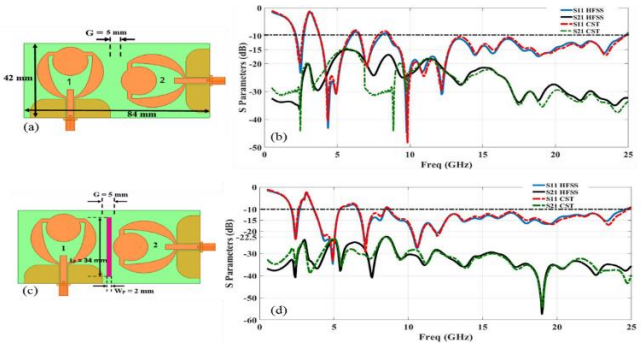

Fig. 4. 2 × 1 MIMO antenna configuration and simulation results, (a) and (b) without parasitic element, (c) and (d) with rectangular strip parasitic element.

TABLE I
Physical Dimensions of the Single-element Antenna as Shown in Figure 1

Parameter	WL	Wg	Lg	Wf	LfWd	Ws	Rs	RL
Value (mm)	42	42	16	10.7	3	160.5	208	15

The simulation results for the single-element antenna are shown in Fig. 3, in which HFSS and CST confirm the multiband performance of the structure.

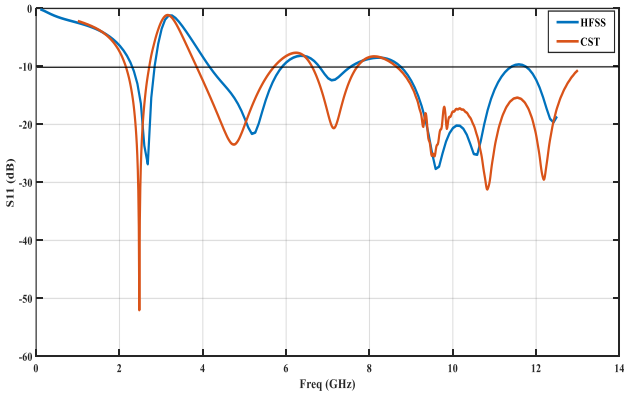

Fig. 3. Return loss simulation of the single-element antenna

3. 1 × 2 MIMO Antenna Design

In the design of a MIMO antenna, it is essential to consider the fringing effect at the patch edges. The electric fields generated between the patch and the ground plane lead to edge effects, resulting in an increased interaction between the electric fields at the patch-ground plane interface. This causes the patch to appear larger when viewed from the ground plane side. The effective dielectric constant, ε, is used to account for the fact that the electric field in a microstrip antenna does not experience the full permittivity of the substrate material, which is calculated as:

$$\varepsilon_{reff} = \frac{\varepsilon_r + 1}{2} + \frac{\varepsilon_r - 1}{2}\left[1 + 12\frac{h}{W}\right]^{-0.5} \quad , \quad \frac{W}{L} \geq 1 \qquad (1)$$

In which ε_r is the relative permittivity (dielectric constant) of the substrate, h is the height (thickness) of the substrate, and W is the width of the microstrip line.

A commonly used formula for the effective length L_{eff} :

$$\Delta L = 0.412h\frac{(\varepsilon_{reff} + 0.3)(\frac{W}{h} + 0.264)}{(\varepsilon_{reff} - 0.258)(\frac{W}{h} + 0.8)} \qquad (2)$$

$$Leff = L + \Delta L \qquad (3)$$

Where L is the physical length of the patch, ΔL is the length extension caused by the fringing fields.

In the design of MIMO antennas, two primary factors must be considered to achieve optimal performance. First, the antenna design should maximize spatial diversity, which enhances the system's ability to overcome fading and interference. Second, it is essential to maximize the signal-to-noise ratio (SNR), which directly impacts the quality and reliability of the received signal. To optimize spatial diversity, antenna elements should be strategically spaced to minimize mutual coupling and preserve uncorrelated signals between elements. However, in portable communication systems, where space constraints are a significant concern, there is a trade-off between maximizing diversity and minimizing the physical size of the system. This necessitates placing the antenna elements closer together, which can increase mutual coupling and reduce diversity if not properly managed. One approach involves using antenna elements with different radiation patterns or polarizations to reduce correlation between the signals received by each element. By carefully selecting elements with diverse radiation characteristics, an optimal diversity gain can be achieved. Furthermore, the placement of antenna elements must be carefully optimized to minimize mutual coupling and ensure that the correlation between the radiation patterns of the elements is as low as possible. Effective design strategies often incorporate decoupling techniques, such as using parasitic elements, feed networks, or optimizing element orientation, to mitigate the negative effects of mutual coupling and maximize overall antenna performance.

To achieve the maximum SNR in a MIMO antenna, the transmitting antenna should direct its full power toward the receiving antenna. Similarly, the receiving antenna must be capable of capturing the maximum possible power from the transmitting antenna.

Following the assessment of the necessary requirements for MIMO antenna design, we proceed to examine and design two MIMO antenna models in 1×2 and 2×2 configurations. Given the minimal spacing between the MIMO antenna elements, it is crucial to achieve low mutual coupling and maintain isolation between the antenna ports to ensure optimal MIMO performance.

For the 1×2 MIMO design, as shown in Fig. 4 (a), two single-element antennas are arranged orthogonally without any additional isolating structures. To maintain a compact form factor, the antenna elements are positioned as close as possible, with a spacing of 5 mm between them, resulting in an overall compact antenna size. As shown in Fig. 4(b), the simulation results of the MIMO antenna in HFSS and CST software reveal that the isolation between the antenna elements, despite their orthogonal arrangement, is approximately 15 dB. This isolation is attributed to the excitation of the antenna's conductive components by the currents induced by the adjacent antenna element.

One of the effective methods for reducing mutual coupling and enhancing isolation in MIMO antennas, especially when the antenna elements are placed in close proximity to each other, is the use of parasitic elements in the antenna design. Parasitic elements are also used for other purposes, such as changing the antenna's radiation patterns, increasing bandwidth, and extending the operational frequency range of antennas. Incorporating a parasitic element for a MIMO antenna leads to the creation of two induced currents on antenna B when antenna A is excited. The first current results from direct coupling caused by the excitation of antenna A, while the second current is due to the induction from the parasitic element on antenna B. The induced current on the parasitic element, which is generated by the excitation of antenna A, is 180 degrees out of phase with the induced current on antenna A. The induced current on antenna B from the parasitic element is 180 degrees out of phase with the current on the parasitic element itself. As a result, the induced current on antenna B from the parasitic element aligns in phase with the original excitation current from antenna A, resulting in the same direction. This means that the coupling current from the parasitic element to antenna B, along with the induced current from the excitation of antenna A, can cancel each other out. Therefore, when a parasitic element is used, the coupled current from antenna A to antenna B is significantly weakened. The dimensions and length of the parasitic element used in the MIMO antenna configuration are inversely related to the design frequency of the antenna. Specifically, as the antenna design frequency decreases, the length and dimensions of the parasitic element increase. So, the parasitic element in the MIMO configuration reduces the mutual coupling and enhances isolation between the MIMO antenna elements.

As shown in Fig. 4 (c), the parasitic element acts as a decoupling structure between the two antenna elements and is placed as a rectangular strip in the gap between the two elements of the MIMO antenna. The dimensions of this rectangular strip are 2 × 34 mm. As illustrated in Fig. 4(d), the isolation between antennas is reduced up to -22.7 dB.

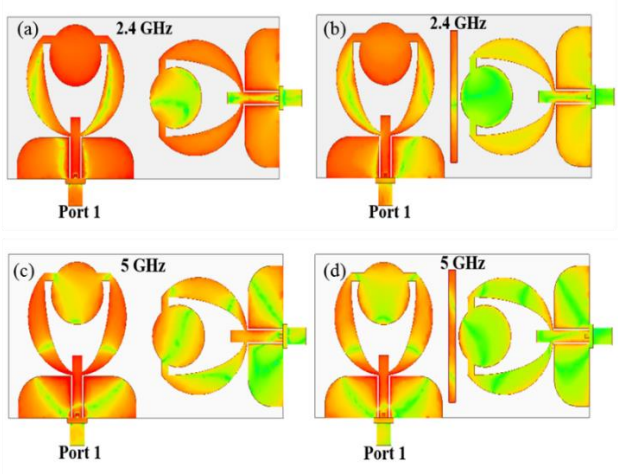

Fig. 5. Surface current distribution at 2.4 GHz and 5 GHz, (a) and (c) without parasitic element and (b) and (d) with parasitic element.

To better understand the effect of the parasitic element, the surface current distribution is studied when port 1 of the antenna is excited and port 2 is terminated with a 50Ω load. The effectiveness of the parasitic element structure used in the MIMO antenna design can be observed in Fig. 5 at 2.4 GHz and 5 GHz, comparing the cases with and without the parasitic element. It can be seen that, in the absence of the parasitic element, strong induced currents flow from antenna 1 to antenna 2, resulting from the inductive behavior exhibited by the conductive structures in response to neighboring current sources. However, when a parasitic element is used as a separator between the two elements, the induced current from antenna 1 to antenna 2 is reduced. This is because the parasitic element minimizes the flow of induced currents from the current-generating antenna to the other elements.

The characteristics of spatial diversity in wideband MIMO antennas are studied using parameters such as DG (Diversity Gain), ECC (Envelope Correlation Coefficient), and TARC (Total Active Reflection Coefficient). **ECC** is a key parameter used to assess the spatial diversity and performance of MIMO antenna systems. It quantifies the degree of uncorrelation between the signals received by the antenna elements, which is crucial for maximizing the spatial diversity gain in MIMO systems. In the ideal case, ECC equals zero, while the practical value is typically less than 0.5. ECC is defined as;

$$ECC = \frac{|S_{11}^{*}S_{12}+S_{21}^{*}S_{22}|}{(1-|S_{11}|^{2}+|S_{21}|^{2})(1-|S_{22}|^{2}+|S_{12}|^{2})} \quad (4)$$

DG measures the increase in overall system performance due to the diversity introduced by multiple antennas in a MIMO system. It reflects the ability of the system to combat fading, interference, and other signal impairments by utilizing independent signal paths from different antenna elements. A high DG value indicates good spatial diversity, meaning the signals received from multiple antennas are sufficiently independent, which improves the overall signal quality and resilience to fading. Ideally, DG should approach 10 dB. DG is defined as;

$$DG = 10\sqrt{1-|ECC|^{2}} \quad (5)$$

TARC is a parameter used to measure the overall isolation between different antenna elements or ports in a MIMO (Multiple-Input Multiple-Output) system. It quantifies how much of the signal is reflected back due to the interaction between the antenna elements, giving insight into the coupling between the ports of the antenna. In the context of MIMO antennas, a low TARC value indicates good isolation between the antenna ports, which is desirable for minimizing interference and maximizing the spatial diversity.

In Fig. 6, the performance of the 2×1 MIMO antenna is investigated through the ECC, DG, and TARC values. As it is observed, the ECC value is less than 0.005, the DG value exceeds 9.9 dB, and the TARC value is less than 5 dB across the frequency band of 2.17 GHz to 24.85 GHz. These values are in accordance with engineering standards and demonstrate the excellent diversity performance of the designed MIMO antenna.

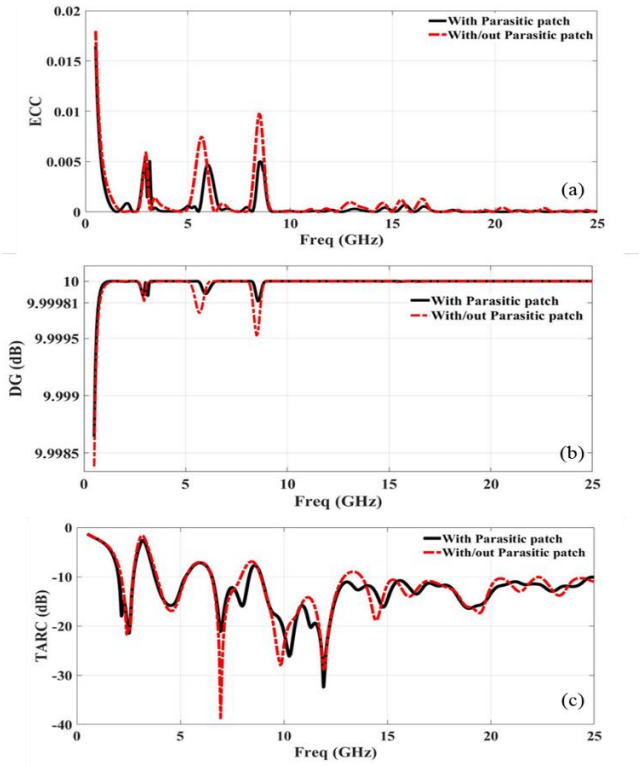

Fig. 6. Effect of parasitic element on 2×1 MIMO antenna, (a) ECC, (b) DG, and (c) TARC value.

III. FABRICATION AND MEASUREMENT RESULTS

After confirming the performance of the designed antenna, the fabrication and testing were carried out in a laboratory environment. The fabricated single-element antenna is shown in Fig. 7. The S-parameters of the prototype were measured using an Agilent 8722ES Network Analyzer. For measuring the antenna's maximum gain, a well-calibrated horn antenna was used as the reference, while the fabricated prototype served as the receiving antenna. The maximum gain was determined by rotating the antenna in various directions to capture the peak performance. The measurement and simulation results of return loss and gain are presented in Fig. 8. The maximum gain of the antenna remains stable and consistent at around 5 dB across the entire operating bandwidth. Moreover, the simulation and measurement results are in acceptable agreement for both the return loss and gain value.

Fig. 7. fabrication of the single-element antenna

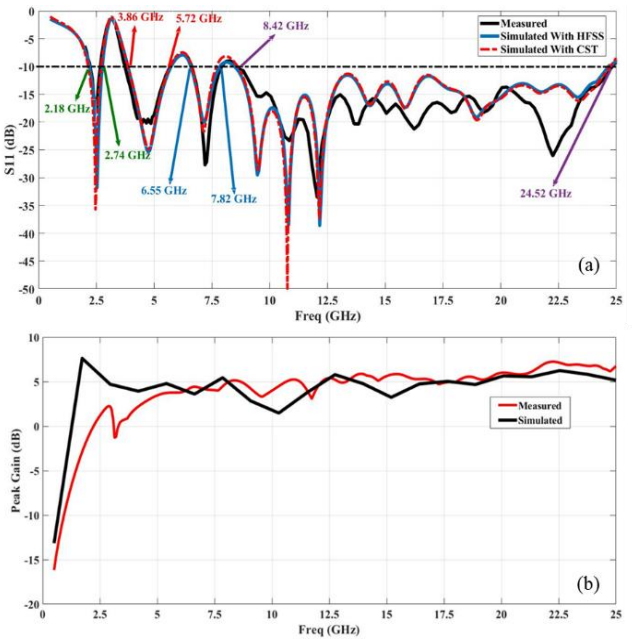

Fig. 8. Simulation and measurement results of single-element antenna (a) return loss and (b) gain value.

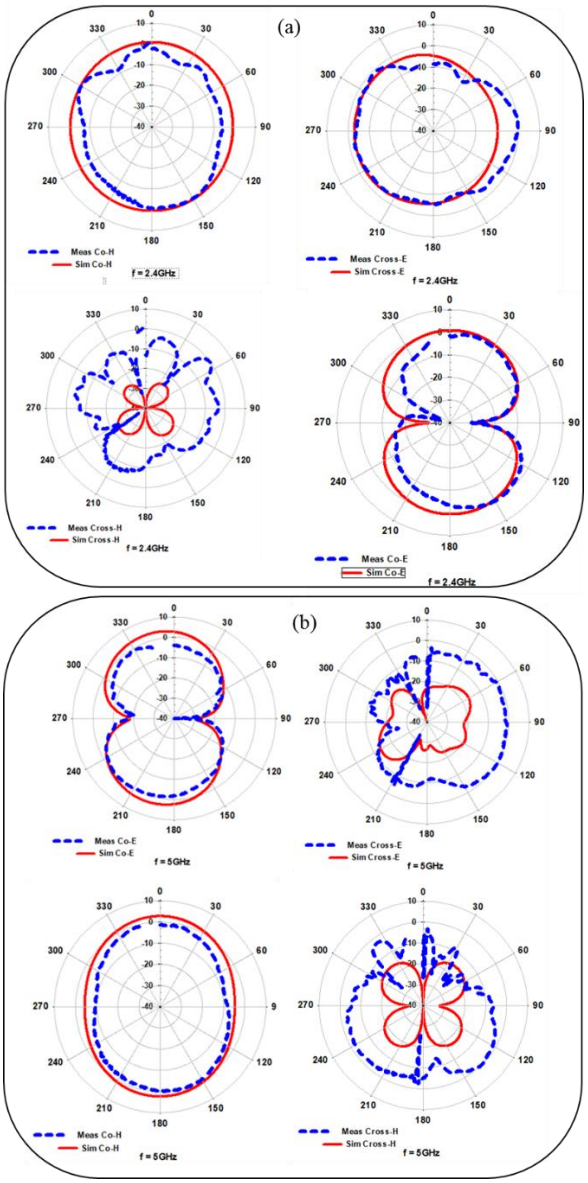

Fig. 9. The simulated and measured radiation patterns of the single-element antenna, (a)2.4 GHz and (b)5 GHz

The measured and simulated radiation patterns of the single-element antenna in the H and E planes at frequencies of 2.5 GHz and 5 GHz are shown in Fig. 9. Based on the images, the measured results confirm the values obtained from the simulations. As evident from the antenna's radiation pattern, the designed single-element antenna exhibits an omnidirectional radiation pattern in the E-plane. For the H-plane, the antenna displays a dipole-like radiation pattern. At frequencies of 2.4 GHz and 5 GHz, the antenna demonstrates a stable and uniform radiation pattern, confirming its consistent performance.

Fig. 10 illustrates the fabricated prototype of the designed 1×2 MIMO antenna.

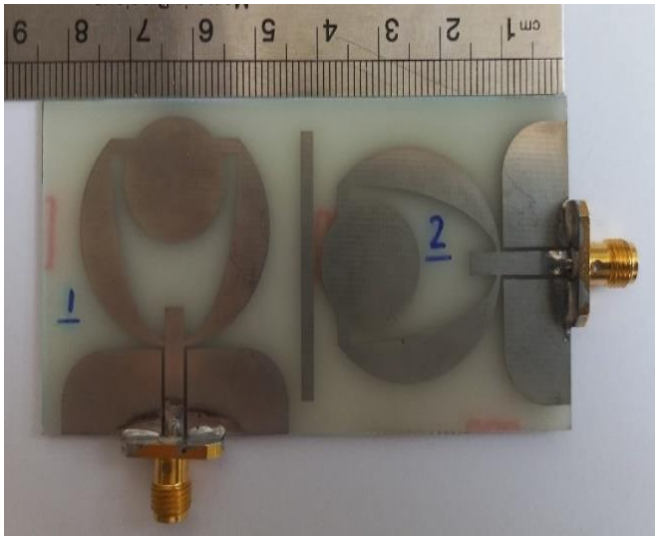

Fig. 10. fabricated 1×2 MIMO antenna

The simulated and measured results for the antenna's S-parameters (S_{11} and S21) are shown in Fig. 11. The simulated data, obtained using CST and HFSS software, as well as the measured data, exhibit consistent and comparable behavior. As depicted in Fig. 11, the impedance bandwidth of the antenna, defined by $|S_{11}|<-10$ dB, ranges from 2.17 GHz to 24.85 GHz (except for notch bands). This indicates good impedance matching across the operational bands. The measured impedance bandwidth spans four working bands: 2.17 – 2.62 GHz, 3.6 – 5.42 GHz, 6.68 – 8.42GHz, and 8.85 – 24.85 GHz. These bands enable compatibility with several communication standards, such as Wi-Fi, Bluetooth, LTE, IEEE 802.11 a/b/g/n, and wireless systems operating in X-band and Ku-band.

As shown in Fig. 11(b), the measured isolation between antenna elements is greater than 21.6 dB across the entire impedance bandwidth. The use of the proposed parasitic element significantly improves isolation, achieving a minimum isolation of over 21 dB. This ensures consistent and reliable performance throughout the operational bands. The maximum gain of the antenna is depicted in Fig. 11(c). For the frequency range of 2.17 – 24.85 GHz, the measured gain varies between 3.9 dB and 6.9 dB, showing stable performance with minimal fluctuation. Compared to the single-element antenna, the gain of the MIMO antenna has increased. This improvement can be attributed to the redistribution and constructive combination of radiated energy across multiple elements in the MIMO system. The observed gain is suitable for Ultra-Wideband (UWB) applications. It is observed that the simulation results closely match the measured results, demonstrating strong agreement between the two. However, a slight discrepancy is present in certain bands, which can be attributed to fabrication tolerances and losses in the connectors.

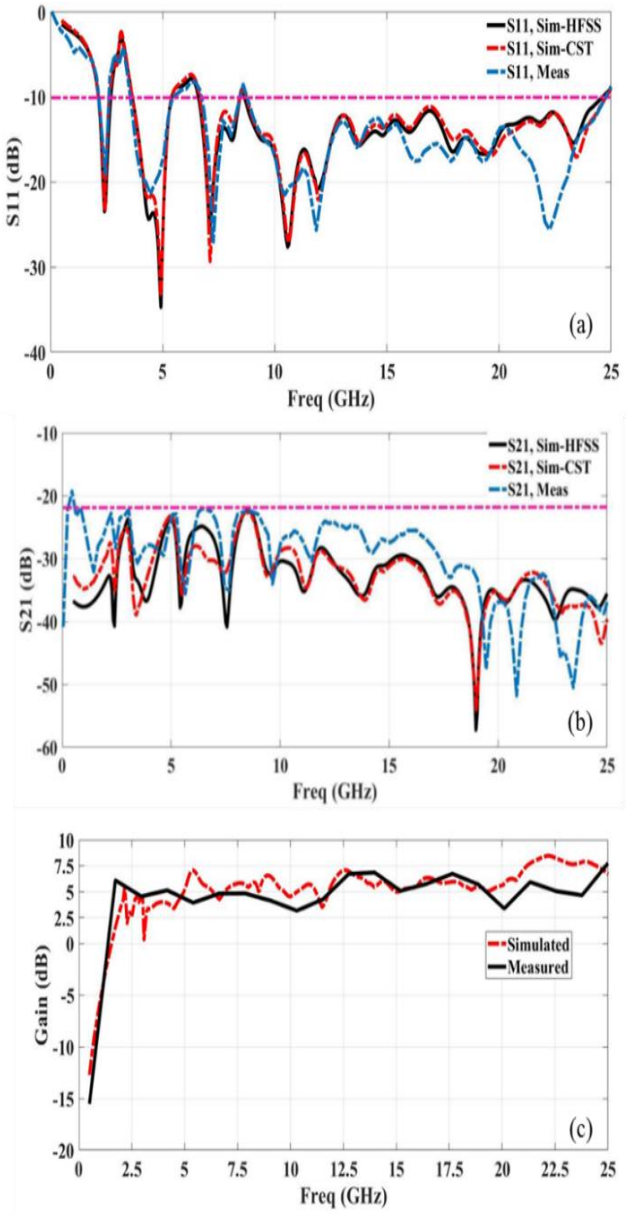

Fig .11 Measured and simulated results of 1×2 MIMO antenna, (a) S_{11}, (b) $S_{21,}$ and (c) gain.

Fig. 12 (a) and (b) depict the radiation patterns of the antenna for both H-plane and E-plane at frequencies of 2.4 GHz and 5 GHz while port 1 of the antenna is excited, and port 2 is terminated with a 50Ω load. It can be observed that the simulated and measured radiation patterns of the antenna exhibit good agreement. The proposed antenna demonstrates a stable omnidirectional radiation pattern in the E-plane and a bidirectional pattern in the H-plane at the tested frequencies. This type of radiation pattern satisfies the requirements of communication systems that demand omnidirectional coverage.

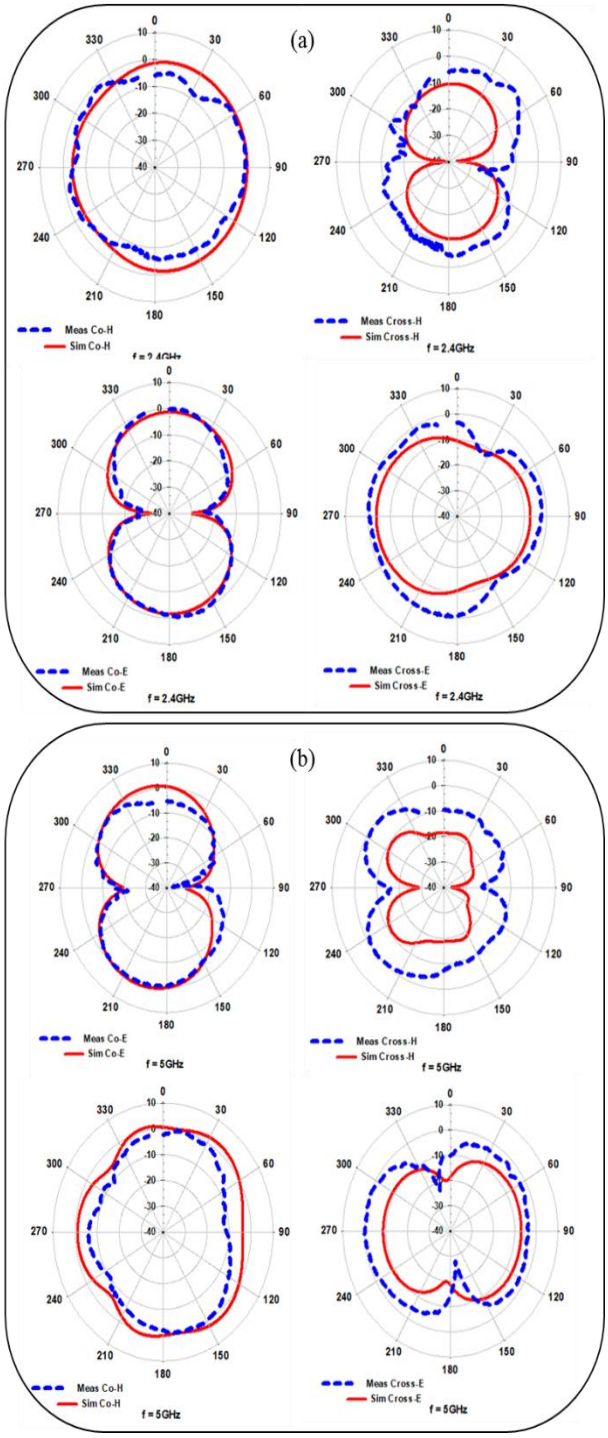

Fig. 12. The simulated and measured radiation patterns of the 1×2 antenna, (a)2.5GHz and (b) 5GHz

IV. Conclusions

A MIMO antenna design has been successfully proposed and verified through simulation and experimental measurements. The antenna achieves wideband performance with four distinct operating bands, demonstrating excellent impedance matching and stable radiation characteristics. The inclusion of a parasitic element significantly enhances port-to-port isolation, reducing mutual coupling to levels exceeding 21 dB. The maximum measured gain is stable across the bands, ranging from 3.9 dB to 6.9 dB, with omnidirectional and bidirectional patterns in the E-plane and H-plane, respectively. These characteristics make the antenna ideal for applications in Bluetooth, Wi-Fi, LTE, and other wireless communication standards. The close alignment between simulation and measurement results validates the design methodology, although minor discrepancies are attributed to fabrication imperfections and connector losses. Future work could explore further miniaturization and integration into more compact systems while maintaining performance.

References

[1] Malviya L, Panigrahi RK, Kartikeyan MV. MIMO antennas for wireless communication: theory and design. CRC Press; 2020 Dec 15.
[2] Jensen MA, Wallace JW. A review of antennas and propagation for MIMO wireless communications. IEEE Transactions on Antennas and propagation. 2004 Nov 8;52(11):2810-24.
[3] Yan S, Soh PJ, Vandenbosch GA. Dual-band textile MIMO antenna based on substrate-integrated waveguide (SIW) technology. IEEE Transactions on antennas and propagation. 2015 Sep 7;63(11):4640-7.
[4] Sree GN, Babu KV, Das S, Islam T. Design and optimization of a deep learning algorithm assisted stub-loaded dual band four-port mimo antenna for sub-6 ghz 5g and x band satellite communication applications. AEU-International Journal of Electronics and Communications. 2024 Feb 1;175:155074.
[5] Francis F, Rosaline SI, Kumar RS. A broadband metamaterial superstrate based MIMO antenna array for sub-6 GHz wireless applications. AEU-International Journal of Electronics and Communications. 2024 Jan 1;173:155015.
[6] Hasan MM, Islam MT, Alam T, Alzamil A, Soliman MS. Electromagnetic coupling shielding in compact MIMO antenna using symmetric T-shaped metamaterial structure for 5G communications. Optics & Laser Technology. 2024 Feb 1;169:110046.
[7] Zhai G, Chen ZN, Qing X. Enhanced isolation of a closely spaced four-element MIMO antenna system using metamaterial mushroom. IEEE Transactions on Antennas and Propagation. 2015 May 18;63(8):3362-70.
[8] Zou XJ, Wang GM, Kang GQ, Song W, Tan M, Xu XG, Zhu H. Wideband coupling suppression with neutralization-line-incorporated decoupling network in MIMO arrays. AEU-International Journal of Electronics and Communications. 2023 Jul 1;167:154688.
[9] Qian K, Zhao L, Wu KL. An LTCC coupled resonator decoupling network for two antennas. IEEE Transactions on Microwave Theory and Techniques. 2015 Aug 18;63(10):3199-207.
[10] Wu T, Wang MJ, Chen J. Decoupling of MIMO antenna array based on half-mode substrate integrated waveguide with neutralization lines. AEU-International Journal of Electronics and Communications. 2022 Dec 1;157:154416.
[11] Yousef BM, Ameen AM, Desai A, Hsu HT, Dhasarathan V, Ibrahim AA. Defected ground structure-based wideband circularly polarized 4-port MIMO antenna for future Wi-Fi 6E applications. AEU-International Journal of Electronics and Communications. 2023 Oct 1;170:154815.
[12] Xing H, Wang X, Gao Z, An X, Zheng HX, Wang M, Li E. Efficient isolation of an MIMO antenna using defected ground structure. Electronics. 2020 Aug 6;9(8):1265.
[13] Srividhya K, Jothilakshmi P. Compact coradiator dual polarized MIMO antenna for future 5G, emerging 6G and IoT applications. Engineering Science and Technology, an International Journal. 2024 Mar 1;51:101609.
[14] Khan R, Al-Hadi AA, Soh PJ, Isa CM, Ali MT, Khan S. Dual polarized antennas with reduced user effects for LTE-U MIMO mobile terminals. AEU-International Journal of Electronics and Communications. 2019 Nov 1;111:152880.
[15] Hassan MM, Rasool M, Asghar MU, Zahid Z, Khan AA, Rashid I, Rauf A, Bhatti FA. A novel UWB MIMO antenna array with band-notch characteristics using parasitic decoupler. Journal of Electromagnetic Waves and Applications. 2020 Jun 12;34(9):1225-38.
[16] Cai Y, Cheng G, Ren X, Wu J, Ren H, Song K, Huang Z, Wu X. Highly Isolated Two-Elements Ultra-Wideband MIMO Fractal Antenna with Multi Band-Notched Characteristics. Progress in Electromagnetics Research C. 2021 Nov 1;116.
[17] Abbas A, Hussain N, Sufian MA, Jung J, Park SM, Kim N. Isolation and gain improvement of a rectangular notch UWB-MIMO antenna. Sensors. 2022 Feb 14;22(4):1460.
[18] Liu L, Cheung SW, Yuk TI. Compact MIMO antenna for portable UWB applications with band-notched characteristics. IEEE transactions on antennas and propagation. 2015 Feb 24;63(5):1917-24.
[19] Naeem U, Iqbal A, Shafique MF, Bila S. Efficient design methodology for a complex DRA-SIW filter-antenna subsystem. International Journal of Antennas and Propagation. 2017;2017(1):6401810.
[20] Yang H, Xi X, Zhao Y, Tan Y, Yuan Y, Wang L. Compact slot antenna with enhanced band-edge selectivity and switchable band-notched functions

for UWB applications. IET Microwaves, Antennas & Propagation. 2019 Jun;13(7):982-90.
[21] Li H, Liu J, Wang Z, Yin YZ. Compact 1× 2 and 2× 2 MIMO antennas with enhanced isolation for ultrawideband application. Progress In Electromagnetics Research C. 2017;71:41-9.
[22] Ren J, Hu W, Yin Y, Fan R. Compact printed MIMO antenna for UWB applications. IEEE antennas and wireless propagation letters. 2014 Jul 29;13:1517-20.
[23] Liu L, Cheung SW, Yuk TI. Compact MIMO antenna for portable devices in UWB applications. IEEE transactions on antennas and propagation. 2013 May 15;61(8):4257-64.

[24]10.22075/mseee.202533301.1145
https;//doi.org/10.1002/mop.31151
http;//doi.org/10.1002/mop.30864

Mohamad Hossein Montazerifar Ph.D student in the field of electricity and telecommunications, field and telecommunications field, Islamic Azad University, Mashhad Branch {ma.c}. IEE membership. He was a student at Amirkabir University, Tehran, Iran. He is the head of the education office in Mashhad, Iran. At the 8th Electrical Conference in Khajeh Nasir Toosi, Tehran, he received a paper award in 1375.

Jasem Jamali, Assistant professor, faculty of electrical engineering, Islamic Azad University, Kazeroun Branch. He was a student at Islamic Azad University, Tehran branch. Dr. Jamali was a recipient of the International Association of Geomagnetism and Aeronomy Young Scientist Award for Excellence in 2008 and the IEEE Electromagnetic Compatibility Society Best Symposium Paper Award in 2011.

Zahra Adelpour, Assistant Professor, Faculty of Electrical Engineering, Islamic Azad University, Shiraz branch. She is a university teacher in Shiraz, Fars, Iran, and was a student at Amirkabir University in Tehran, Iran.